W-band Radar aboard of Unmanned Aerial System for Wire Strike Avoidance

Lapo Miccinesi
Department of Information Engineering, University of Florence.
IEEE member
Firenze, Italy
lapo.miccinesi@unifi.it

Luca Bigazzi
Department of Information Engineering, University of Florence.
Firenze, Italy
luca.bigazzi@unifi.it

Alessandra Beni
Department of Information Engineering, University of Florence.
IEEE student member
Firenze, Italy
alessandra.beni@unifi.it

Massimiliano Pieraccini
Department of Information Engeenering – University of Florence.
IEEE member
Firenze, Italy
massimiliano.pieraccini@unifi.it

***Abstract*— Wire strikes pose a serious threat for small UAS flying below 120 m, as wires are difficult to detect with the onboard visual system. In this paper we experimentally tested the capability of a W-band miniaturized radar as wire strike avoidance system for a small UAS in autonomous operation. The radar successfully detected the wire and the UAS was able to change its trajectory according to the position of the wire retrieved by the radar, in all tests we performed.**

Keywords— avoidance system, radar, unmanned aerial vehicle (UAS), wire detection, wire strike.

I. Introduction

Wire strikes are a serious threat to all low altitude aerial vehicles: worldwide power lines claim an average of 2 helicopter strikes every week [1]. There are no official statistics on wire strikes of small unmanned aerial systems (UAS), but surely, they are many hundreds or, more likely, thousands each year. Small UASs fly below 120 m, where collisions with wires are more probable. Furthermore, wires are hard to detect with onboard cameras, especially when the wire does not stand out against the sky.

Helicopters are often equipped with special sensors: Powerline Detection System [2], lidar [3,4], radar [5,6]. But the same equipment could be too expensive, bulky, and heavy to be used aboard a small UAS. This is why specific technical solutions for small UAS must be developed.

Small UASs can use their own camera to detect wires but to automatically recognize a wire can be a rather complex problem [7]. Lidars have also been proposed [8], however, they may be more suitable for large UAS. As automotive anti-collision systems W-band radars are increasingly popular, small, and inexpensive, their application as wire strike avoidance system is currently a viable solution. This kind of sensor has already been proposed and tested for mapping [9] and as a collision avoidance system in cooperation with a stereoscopic camera [10].

The aim of this paper is to test the capability of a miniaturized W-band radar (originally designed for automotive applications) to operate as wire strike avoidance system for an UAS in autonomous flight. Because of the small size of a suspended electric wire, this is not obvious. Despite that, the UAS was able to detect the wire and to change the trajectory according to the programmed path in all tests we performed.

This research was co-funded by Horizon 2020, European Community (EU), AURORA (Safe Urban Air Mobility for European Citizens) project, ID number 101007134.

II. Avoidance System

Fig. 1 shows the equipment used for wire strike avoidance. A DJI Matrice 300 RTK [11] was equipped with an AWR1843BOOST radar by Texas Instruments [12], and with a Jetson board computer by NVIDIA. The obstacle avoidance algorithm runs on the Jetson board, which is connected to the radar via a USB port. Moreover, the Jetson is connected to the UAS via UART protocol, which enables the computer to pilot the UAS. As aforementioned, this equipment has been preliminary tested for obstacle detection and avoidance in [9,10].

In Fig. 1, the on-board computer was located on the top of the UAS, and the radar (at the bottom) was aimed in the forward direction of the UAS. The on-board computer uses the telemetry provided by the UAS and the detected targets to elaborate a map of its environment [9].

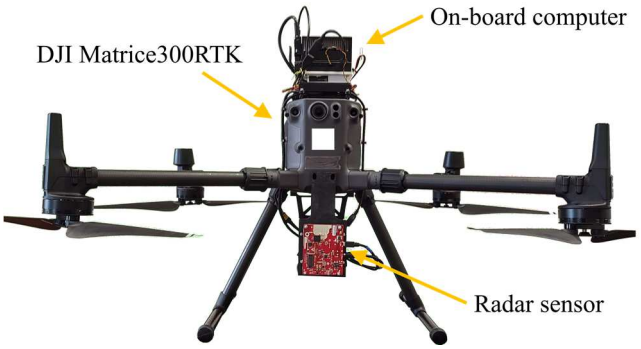

Fig. 1. Equipment used for testing the wire strike avoidance.

A. The radar

The radar provides a continous wave frequency modulated (FMCW) signal starting from 77 GHz with 300 MHz of bandwidth and 256 time-samples, which correspond to 0.5 m of resolution and 120 m of maximum range. The radar is a multiple input multiple output (MIMO) provided with 3 serial transmitting (TX) and 4 receiving (RX) antennas. The 12 virtual antennas are arranged as shown in Fig. 2 (the z axis represents the altitude, while the x axis is left to right, and λ is the wavelength of the electromagnetic signal). The colours identify which TX antenna has to be switched on for obtaining the specified virtual antenna. Since the elevation resolution is poor (about 30°), the elevation of the target measured by the radar is not used for mapping, and it is set equal to zero for

each target. Setting the elevation equal to zero is equivalent to assuming each detected target in the horizontal plane at the same altitude of the UAS. This assumption is not as restrictive as it seems since targets at the same altitude as the UAS are usually the most reflective. Anyhow, the elevation-resolution is used as a field of view (FOV) cut-off to reject targets outside a selected elevation angle. The angular FOV was $\pm 45°$ in azimuth and $[0°, 20°]$ in elevation. The targets outside these intervals are not used for mapping.

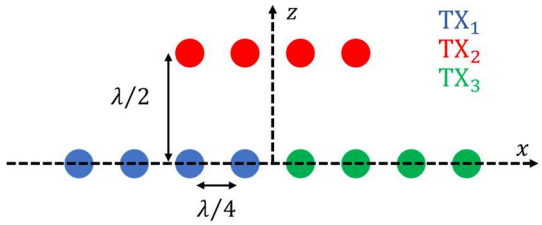

Fig. 2. Virtual antenna position of AWR1843BOOST [14].

To reduce the false alarms, the data of each radar frame have been processed with a constant false alarm rate (CFAR) algorithm [9,13,14]. The block scheme of this algorithm is shown in Fig. 3. The fast Fourier transform (FFT) is calculated along the range direction and the result is arranged in a matrix without considering the antenna position. Then, FFT is calculated along the long-time (Doppler FFT). The range and Doppler CFAR have been evaluated separately. We used a cell-averaging (CA-CFAR) in Doppler a cell-averaging smallest of-CAFAR (CASO-CFAR) in range [13,14]. CA-CFAR is the most effective algorithm for detecting wires, but it could fail to detect extended target (e.g. the crown of a tree), so for safety reasons we implemented the CASO-CFAR in range. The information of range and Doppler CFAR are combined, and the position of the detected targets is estimated by using the angular information given by the spatial distribution of MIMO. For each target that exceeds the CFAR thresholds, the algorithm provides the position, speed, signal to noise ratio and noise floor. The position has been used for mapping the environment in front of the UAS as described in [9,10].

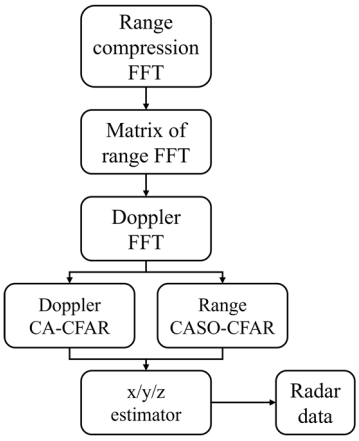

Fig. 3. CFAR algorithm.

B. *The obstacle detection*

The targets discriminated by the CFAR algorithm are mapped into a map which considers the UAS position (provided by a global navigation satellite system (GNSS)) and the attitude. Clearly, not all targets can be considered as obstacles, for example those that are distant from the UAS trajectory. Moreover, it is not necessary to look for obstacles outside the FOV of the radar. To reduce the complexity of the searching algorithm, we define a safety region, in which the presence of obstacles is sought starting from the furthest distance. When an obstacle is detected, the on-board computer triggers the decommitment strategy: the UAS lifts up until the obstacle is no longer visible, after that the drone continues the mission at the new altitude. Fig. 4 shows a scheme of the searching region during the obstacle detection task.

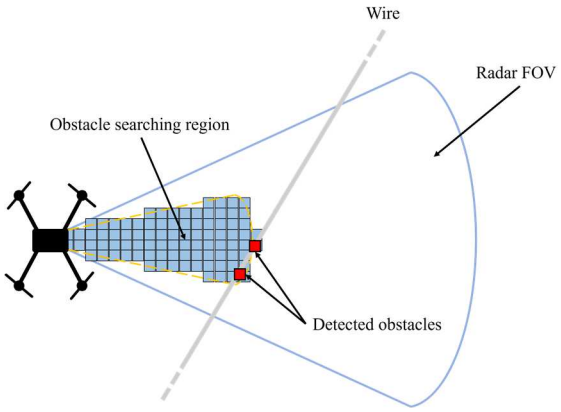

Fig. 4. Scheme of obstacle detection algorithm.

C. *The obstacle avoidance framework*

The on-board computer runs robot operating system (ROS) [15]. ROS is a software framework able to simplify the development of robotic applications: it allows to manage separate parts of code and to permit their intercommunication. ROS can schedule different applications and tasks, named nodes which could share variables, named topics, between each other. Fig. 5 shows a block scheme of software framework. The radar node provides the information on the detected obstacles towards a proper topic. The radar data are processed in the obstacle detection system (ODS) node and mapped using Octomap in a map referenced to global coordinates. Since the radar is able to detect few targets per frame, the radar map is generated at a frequency of 5 Hz, even if no targets are detected. In this way, the obstacle detection task is able to provide warning and alarm messages of obstacles detected in advance. When an obstacle is detected, the ODS node provides an alarm message to the control node with the position of the target. The control node plans a new route in terms of velocity and communicate it to the control task inside the DJI on-board software development kit (OSDK) node.

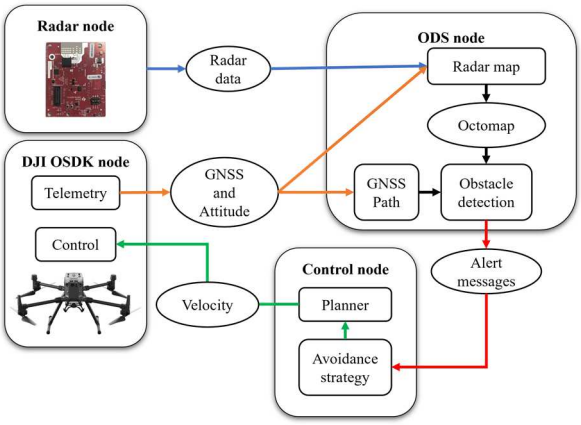

Fig. 5. Scheme of software framework used for obastale avoidance system.

III. Experimental Results

The sensor was tested in a remote area around Firenze, Italy. A satellite image of the area is shown in Fig. 6. A suspended telecommunication wire was along the road. The mission was planned (green line in Fig. 6) in order to have the wire in the radar FOV. We repeated the mission several times to validate the repeatability of the avoidance system in the same scenario. Fig. 7 shows a panoramic image and the FOV camera aboard the UAS. The flights were performed at approximately the same altitude as the cable (4.5 – 5.9 m above the home points), with a speed of 1 m/s. We defined a safety area of 6 m in distance and 24° in azimuth.

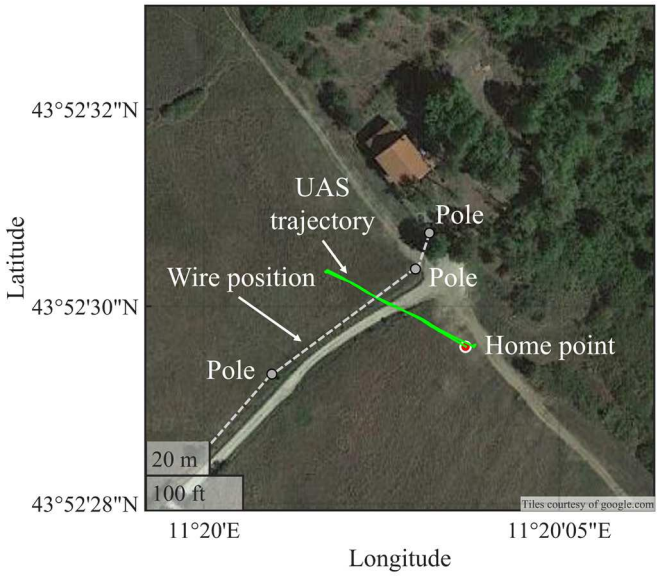

Fig. 6. Satellite image of the testing area.

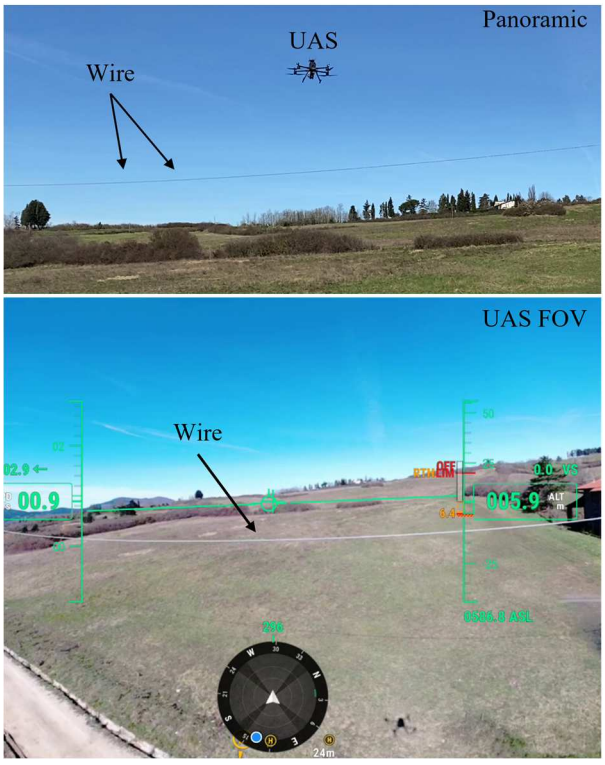

Fig. 7. Panoramic and FOV images of the UAS during the test.

An experimental result of the obstacle avoidance strategy is shown in Fig. 8. The UAS was flying towards the cable; when the obstacle was detected inside the safety area, the decommitment strategy has been actuated. The UAS raised the altitude and continued the mission in the same direction. When the mission is completed the UAS returns to the home point. The other targets (tree and ground) in Fig. 8 were detected during the return to home or landing operation. These targets were not considered as obstacles since they are far from the UAS or far from its trajectory.

Fig. 9 shows the top view of the mission shown in Fig. 6. We can notice that the obstacles are located along the wire, and they are detected on the right with respect to the trajectory. The CFAR algorithm gives priority to the target closest to the radar: as the trajectory was not orthogonal to the wire, most of the detected targets are located on a side (the side closest to the wire). The targets on the left were not detected since the decommitment strategy changed the altitude of the UAS.

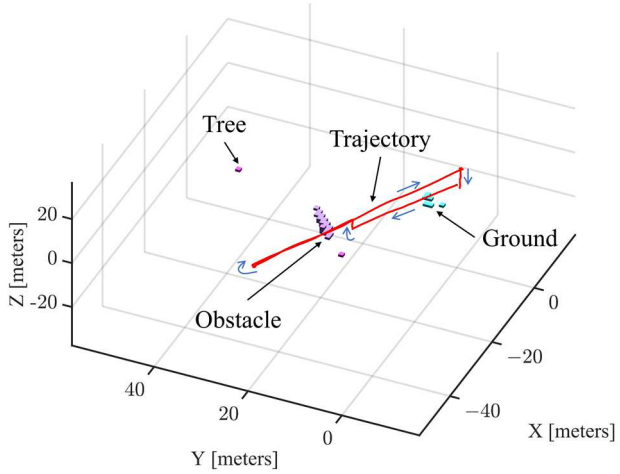

Fig. 8. Example of wire detection and avoidance.

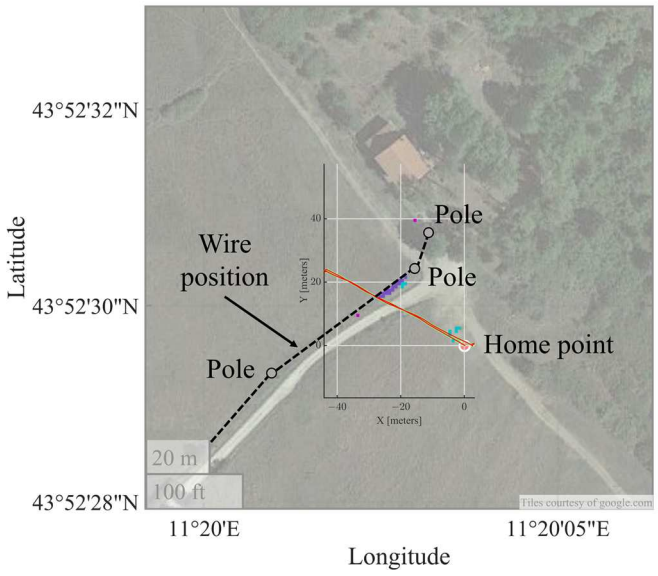

Fig. 9. Top view of an example of wire detection and avoidance.

Fig. 10 shows a detail of the obstacle avoidance strategy during the experimental test. The red line represents the UAS trajectory, and the blue line is the measured position of the target. We can note that the vertical length of the measured position is about 1 m. In fact, while the UAS is lifting up, the wire is still inside the radar FOV and it results as a detected

target in the same plane of the UAS. It is worth to notice that we defined a safety area of 2 m above the last detected target.

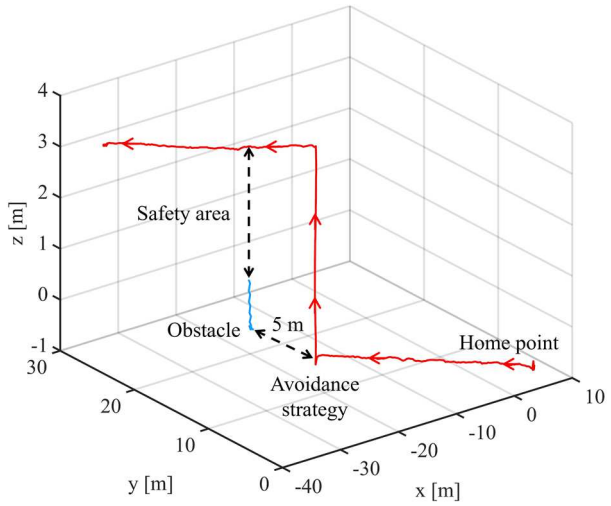

Fig. 10. Example of experitmental of decommitmente strategy during an experimental test.

Finally, Fig. 11 shows the results of 7 missions performed in the same area with different home points and different altitudes. The trajectories are referred to the same reference system. In this image we can notice that the obstacles are detected almost at the same position and the maximum altitude of the UAS is almost the same in each mission.

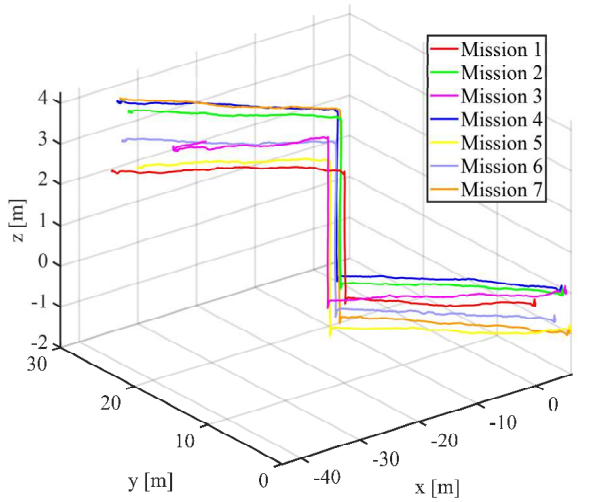

Fig. 11. Trajectories of seven missions which differ from each other in altitude and home point.

IV. Conclusions

In this paper a wire strike avoidance system for small UAS was presented. The system is based on a W-band MIMO radar which is connected to the UAS which was preliminary tested as obstacle avoidance system for generic application [9,10].

The sensor was tested in a realistic scenario with a suspended telecommunication wire. The UAS has been programmed for automatically follow a route and it has been able to successfully detect the wire and to change the trajectory in each test we performed.

A critical limit of this technical solution is that the UAS can detect wires or another obstacle only in front of itself. On the other hand, the UAS elaborates a global map of its environment, so it is enough that before starting going back or to the side, the UAS turns around itself for mapping its surrounding and defining a safety zone. When the UAS reaches the edges of the safety zone, turns around once again and so on. As this UAS is designed to fly autonomously the mission can be easily changed in flight following these criteria.

References

[1] L. Stuart. "A plan for reducing wire strike accidents." *Professional Pilot,* vol. 85, 2012

[2] C. C. Joseph, and K. N. Crocker. "Helicopter electronic system for detecting electric power lines during landing." U.S. Patent No. 5,859,597. 12 Jan. 1999.

[3] K. R Schulz, S. Scherbarth, S., U Fabry, "Hellas: obstacle warning system for helicopters". In: Laser Radar Technology and Applications VII (Vol. 4723, pp. 1-8). SPIE. July, 2002.

[4] R. Sabatini, A. Gardi, S., Ramasamy, M. A. Richardson, "A laser obstacle warning and avoidance system for manned and unmanned aircraft." In: 2014 IEEE Metrology for Aerospace (MetroAeroSpace) (pp. 616-621). IEEE. May, 2014

[5] D. S. Goshi, Y. Liu, K. Mai, L. Bui, Y. Shih, "Cable imaging with an active W-band millimeter-wave sensor." In: 2010 IEEE MTT-S International Microwave Symposium (pp. 1620-1623). IEEE. May 2010.

[6] S. Futatsumori, C. Amielh, N. Miyazaki, K. Kobayashi, and N. Katsura, "Helicopter Flight Evaluations of High-Voltage Power Lines Detection Based on 76 GHz Circular Polarized Millimeter-Wave Radar System", In: 2018 15th European Radar Conference (EuRAD), Sep. 2018, pp. 218–221.

[7] A. A. V. Junior, P. S Cugnasca "Detecting cables and power lines in Small-UAS (Unmanned Aircraft Systems) images through deep learning. In: 2021 IEEE/AIAA 40th Digital Avionics Systems Conference (DASC). IEEE, 2021. p. 1-7.

[8] F. Azevedo, A. Dias, J. Almeida, A. Oliveira, A. Ferreira, T. Santos, A. Martins, E. Silva, "Lidar-based real-time detection and modeling of power lines for unmanned aerial vehicles". *Sensors*, Vol. 19, No. 8, n. 1812 (2019).

[9] L. Miccinesi, L. Bigazzi, T. Consumi, M. Pieraccini, A. Beni, E. Boni, M. Basso, "Geo-Referenced Mapping through an Anti-Collision Radar Aboard an Unmanned Aerial System," *Drones*, vol. 6, no. 3, p. 72, Mar. 2022

[10] L. Bigazzi, L. Miccinesi, E. Boni, M. Basso, T. Consumi, and M. Pieraccini, "Fast Obstacle Detection System for UAS Based on Complementary Use of Radar and Stereoscopic Camera," *Drones*, vol. 6, no. 11, p. 361, Nov. 2022.

[11] Matrice 300 RTK, DJI. https://www.dji.com/matrice-300?site=brandsite&from=nav (accessed Apr. 5, 2023).

[12] AWR1843BOOST Evaluation board. https://www.ti.com/tool/AWR1843BOOST(accessed Apr. 5, 2023).

[13] E. Hyun, W. Oh, J. H. Lee, "Two-Step Moving Target Detection Algorithm for Automotive 77 GHz FMCW Radar," In: 2010 IEEE 72nd Vehicular Technology Conference - Fall*, Ottawa*, ON, Canada, 2010, pp. 1-5.

[14] H. Rohling, "Radar CFAR Thresholding in Clutter and Multiple Target Situations," *IEEE Transactions on Aerospace and Electronic Systems*, vol. AES-19, no. 4, pp. 608-621, July 1983

[15] ROS: Home. https://www.ros.org/(accessed Apr. 5, 2023)..